Desalination and Water Treatment
www.deswater.com

doi:10.5004/dwt.2019.24189

160 (2019) 14–22
August

Investigation of scale inhibitors effect on calcium carbonate nucleation process

Raghda Hamdi[a,*], Mohamed Tlili[a,b]

[a]*Laboratoire de Traitement des Eaux Naturelles, Centre des Recherches et Technologies des Eaux, Technopole Borj Cédria, BP 273 Soliman 8020, Tunisia, email: hamdi.raghda@gmail.com (R. Hamdi)*
[b]*Department of Chemistry, College of Sciences – King Khalid University, 9033 Abha, Saudi Arabia, email: mtlili@kku.edu.sa (M. Tlili)*

Received 7 October 2018; Accepted 26 March 2019

ABSTRACT

Calcium carbonate precipitation has been studied for more than a century. Nevertheless, the early stage of $CaCO_3$ nucleation process still attracts the attention of researchers. In this paper, a new method to investigate the effect of scale inhibitors on this nucleation is presented. It consists on the modeling of the electrical conductivity evolution during $CaCO_3$ precipitation by using a CO_2-degassing method called the fast controlled precipitation method (FCP). Tested inhibitors were sodium polyacrylate (RPI) and sodium-tripolyphosphate (STP). Results shown that nucleation process is governed by two main steps; in the first one ion pairs are formed by the association of Ca^{2+} and CO_3^{2-} ions. The second one consists on the agglomeration of the formed ion pairs to form stable nuclei that can grow. Adding scale inhibitors slowed-down the nucleation rate and affects these two steps, especially the ion pair agglomeration; the ion pair formation and precipitation threshold requires a higher supersaturation coefficients showing that the inhibitor acts on the nucleation process by preventing the association of calcium and carbonate ions and disrupting the aggregation of the formed ion pairs. It was also shown that added chemicals inhibit the homogeneously formed $CaCO_3$ nuclei and affect the micro structure of the precipitate.

Keywords: Calcium carbonate; Scale inhibitor; Nucleation process; Ion pairs

1. Introduction

Calcium carbonate scaling is at the origin of several technical problems in natural water installations: desalination plants, industrial cooling circuits, drinking water distribution systems, etc. For this reason, a number of physical [1,2] and chemical methods for scale prevention have been developed. As chemical method, the inhibition of $CaCO_3$ formation which consists on adding small amounts of mineral or organic chemicals is widely used in particular in industrial circuits. So, a large range of inhibitory substances were shown efficient in the literature including phosphates and phosphonates [3,4], polyacrylates [5,6] and various other polymers and copolymers of carboxylates and sulfonates [7,8].

Scale inhibitors function by one or more closely related mechanisms interfering with the crystallization stages [9]: (i) threshold effect, (ii) crystal distortion and (iii) dispersion. The threshold effect is the ability of an inhibitor to prevent or to delay the precipitation of salts which have exceeded their solubility products at a sub-stoichiometric level and to interact in non-stoichiometric ratios with nucleation sites to limit the growth. Threshold inhibitors can also disrupt the clustering and ordering processes but typically have little crystal distortion or dispersion properties. The crystal distortion affects the ordering and growth reactions. Interference to normal crystal growth produces an irregular crystal structure with poor scale forming ability. The dispersion is the ability of an inhibitor to reduce the agglomeration and the settling of suspended solids. The inhibitor chemisorbs onto the crystal surface giving the crystal a surface charge. Similar charges cause the crystals to repel one other.

Several methods and analytical techniques have been used to highlight the mode of action of inhibitors. Liu et al. [7] have used scanning electronic microscopy (SEM) and

*Corresponding author.

X-ray powder diffraction (XRD) to investigate the effect of polymers. They showed that additives change highly the morphology, micro structure and size of precipitated calcium carbonate crystals. By using the field emission scanning electron microscopy (FESEM), Ruiz-Agudo et al. [3] have proposed as inhibition mechanism, at the earlier stage of $CaCO_3$ formation, that the additive hinders the aggregation of pre-nucleation ions. Insufficient inhibitor amount leads to an aggregation of pre-nucleation clusters at higher supersaturation via amorphous intermediates that later transform into crystalline phases. The formed crystals grow through nonclassical oriented aggregation of nanoparticles that seem to incorporate the copolymer that stabilizes them and prevents merging. This agree with the results of Al Nasser, et al. [10] which showed, using the focused beam reflectance measurement (FBRM) inline monitoring technique, that the inhibitory substance delays the $CaCO_3$ clusters agglomeration. SEM images revealed that the mechanism of inhibition could be a surface adsorption or distortion of inhibitor molecules on the growing calcium carbonate crystals. Adsorption mechanism was also proposed by Yang, et al. [11]. They demonstrated by using XRD, SEM and FTIR techniques that during $CaCO_3$ crystal growth, the inhibitor molecules or ions are adsorbed in a different degree onto the various types of crystal faces, since each type of face has a different surface lattice structure and thus a different distribution of adsorption sites. Lin, et al. [12] proved, using a pH-stat system, that the presence of inhibitors during precipitation can block the active growth sites of the scale surface, thus retarding the growth stage of calcium carbonate precipitation. Moreover Liu et al. [13] showed, using the static and rapid controlled precipitation methods, that the inhibitors could distort the crystal lattice of the precipitates, destroying their compact and regular crystal structures and changing them into loose and rough ones, thus retarding the formation of precipitates. The SEM and XRD analyses confirmed these findings. Greenlee et al. [14] demonstrated that those inhibitors can also decrease the mass of precipitated calcium carbonate by decreasing particle size and modifying the shape of the precipitate. These findings are confirmed by the SEM images. Such inhibitors are principally designed for their ability to form a sufficient number of coordinative bonds with surface cations of nucleating precipitates. That has been shown, using Raman spectroscopy technique, in the case of inorganic phosphate [15] and sodium polyacrylate [16].

A large variety of techniques were used to understand the mode of inhibitors action on calcium carbonate crystallisation. Although the effect of inhibitory substances on the growth step and on the micro structure of $CaCO_3$ is well studied and several mechanisms were presented, few investigations have focused on their effect at the nucleation stage. So, the present work focuses on the effect of chemical substances on the $CaCO_3$ ion pair formation and aggregation at the earlier nucleation stage. For this, our recently developed method [17] for highlighting the role of $CaCO_3°$ ion pairs in the nucleation-growth of calcareous scale was exploited. As inhibitors, polyacrylate and polyphosphate substances were tested. The method consists on modelling the precipitation curves (resistivity *vs* pH) by using the McCleskey model and considering thermodynamic calculations of all equilibrium between different species of $CaCO_3$–CO_2–H_2O system.

2. Material and methods

2.1. Water preparation

The calco-carbonic pure synthetic water CCPW was prepared by dissolving 0.4 g·L^{-1} of solid calcium carbonate in distilled water under CO_2 bubbling according to:

$$CaCO_3 + CO_2 + H_2O \leftrightarrows Ca^{2+} + 2HCO_3^-$$

For all experiments, the initial pH value was adjusted at 5.9 by CO_2 babbling to maintain the work solution under saturated [Ω = 0.25 Eq. (1)]. This supersaturation degree (Ω) with respect to calcite, which is the most stable form of calcium carbonate, is calculated considering the following equation:

$$\Omega_{CaCO_3} = \frac{\left[Ca^{2+}\right]\cdot\left[CO_3^{2-}\right]\cdot\gamma_{Ca^{2+}}\cdot\gamma_{CO_3^{2-}}}{K_{sp}\left(calcite\right)} \quad (1)$$

where γ_i is the ion activity coefficient, *[i]* is the ion concentration and K_{sp}(calcite) is the calcite solubility product.

The ion activity coefficient, γ_i, was estimated using the Davies equation:

$$\log\left(\gamma_i\right) = -Az_i^2\left(\frac{\sqrt{I}}{1+\sqrt{I}} - 0.3I\right) \quad (2)$$

where T is the temperature in K and ε is the dielectric constant of water which is calculated using Malmberg equation:

$$\varepsilon = 87.74 - 0.40008.T + 0.0009398.T^2 - 0.000001411.T^3 \quad (3)$$

and I is the ionic strength calculated according to:

$$I = \frac{1}{2}\sum_{i=1}^{n} c_i z_i^2 \quad (4)$$

where c_i is the concentration and z_i is the charge of the i^{th} ion.

2.2. Scale inhibitors

Two well-known scale inhibitors, organic-sodium salt of polyacrylate $(C_3H_3NaO_2)_n$-and inorganic-sodium triphosphate ($Na_5P_3O_{10}$)-called respectively thereafter RPI and STP were added in the reaction medium before the onset of the precipitation test. Small amounts, which have no significant effect on the solution ionic strength and conductivity, were used. The concentrations of RPI used are 0.2, 4, 14 and 15 ppm. Besides, the concentrations of STP used are 0.1, 0.6, 0.8 and 0.9 ppm.

The structures of RPI and STP are shown in Fig. 1 and their physicochemical characteristics are represented in Table 1.

2.3. The fast controlled precipitation (FCP) experimental set up

The experimental set up of the fast controlled precipitation (FCP) method is given in Fig. 2. The temperature of the experiment was controlled with a water thermostat bath maintained at 30°C. A polytetrafluoroethylene (PTFE) cell was filled with 500 ml of calco-carbonic pure water (CCPW)

RPI

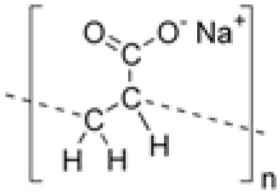

STP

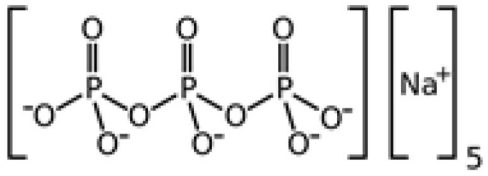

Fig. 1. The structural formulas of scale inhibitors used.

Table 1
The physicochemical characteristics of commercial scale inhibitors used

Scale inhibitors	RPI; sodium poly acrylate	STP; sodium tripoly phosphate
Molecular formula	$(C_3H_3NaO_2)n$	$Na_5P_3O_{10}$
Molecular weight (g/mol)	2000–2300	367.864
Appearance	Clear, slightly yellow liquid	White powder
Density (g/cm³)	1.15	0.8
pH	7.0–7.5	9.2–10.0
Action with water	Soluble	Soluble

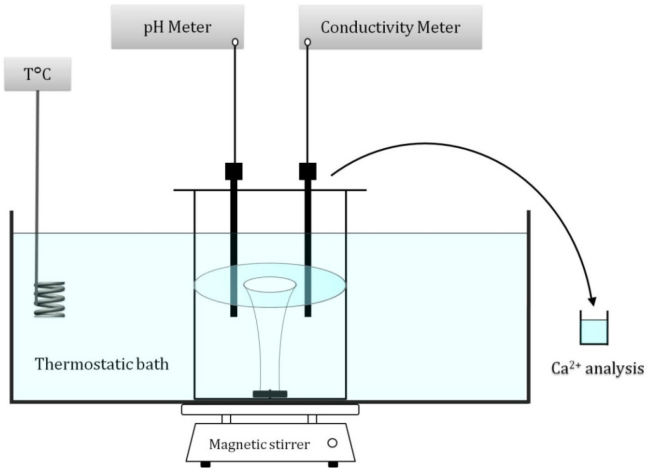

Fig. 2. The fast controlled precipitation (FCP) experimental set up.

which was stirred at 800 rpm. The pH and the resistivity of the solution were continuously recorded, by a pH-meter (Hanna HI 110), and by a conductivity-meter (Meter Lab CDM210). The calcium ion concentration was measured by EDTA complexometry titration.

The FCP method was the subject of numerous recent works [18,19]; its principle is therefore well detailed. It consists in the displacement of the calco-carbonic equilibrium reaction towards calcium carbonate formation by degassing the dissolved carbon dioxide ($CO_{2dissolved}$) from water.

$$Ca^{2+} + 2HCO_3^- \leftrightarrow CaCO_3 + H_2O + CO_{2\ dissolved} \uparrow$$

Degassing occurs on the interface air/water renewed by magnetic stirring, which leads to an increase in the pH values according to the following reactions:

$$CO_{2\ dissolved} \leftrightarrow CO_{2\ atmospheric}$$

$$HCO_3^- \leftrightarrow CO_{2\ dissolved} + OH^-$$

In the FCP reactor $CaCO_3$ precipitates both in bulk solution and on the wall. At the end the FCP test, homogeneously formed precipitate (m_b in gram) can be recuperated by solution filtration with a 0.45 μm pore size cellulose nitrate membrane. By measuring Ca^{2+} amount remaining in the solution, the total precipitated calcium carbonate m_t can be determined. The mass of calcium carbonate m_w heterogeneously formed on the cell wall is then deduced ($m_w = m_t - m_b$) and its rate can be calculated as follow:

$$\%_{hete} = \frac{m_w}{m_t} \times 100 \tag{5}$$

For each FCP test the efficiency is determined. It must incorporate both the nucleation and growth phases. The test time was therefore fixed. The scale inhibition efficiency, E, was then defined by:

$$E(\%) = \frac{\int_0^t (R_{wo} - R_0)dt - \int_0^t (R_w - R_0)dt}{\int_0^t (R_{wo} - R_0)dt} \cdot 100 \tag{6}$$

where R_0 is the initial resistivity, R_{wo} and R_w are the resistivities of water without and with inhibitor at time t, respectively.

2.4. Determination of the nucleation thresholds

The determination of the nucleation thresholds, indicating the beginning of each type of nucleation from a kinetic and thermodynamic point of view, is important given the fact that the formation of $CaCO_3$ in water can take place according to the two mode of nucleation (homogeneous or heterogeneous) [1,20,21].

In order to better delimit the nucleation thresholds, an in-situ measurement of solution conductivity during degasification by agitation was made. In Fig. 3 are reported experimental measurements of pH and resistivity versus time of the solution during the precipitation process. These measurements were carried out on 0.4 g·L^{-1} water

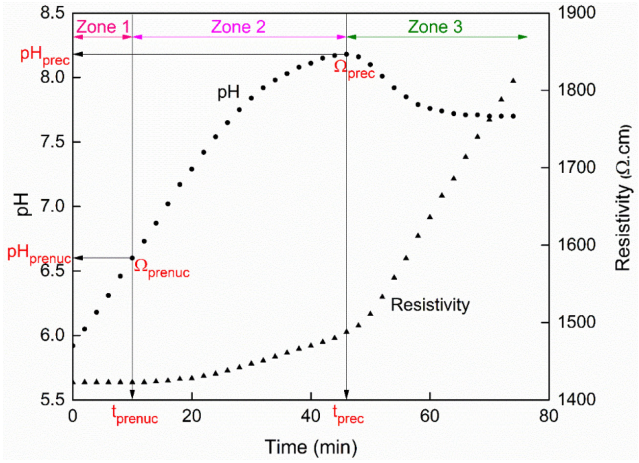

Fig. 3. Temporal evolution of (pH and resistivity) at 800 rpm, 30°C and CCPW0.4 g·L^{-1}.

concentration, at 30°C temperature and 800 rpm stirring speed.

Fig. 3 highlights the limits between three zones:

- *Zone 1:* during the first ten minutes, until the prenucleation induction time "t_{prenuc}" is reached, pH increases and resistivity remains constant. In fact the free ions content does not change.
- *Zone 2*: during the following forty minutes, between t_{prenuc} and t_{prec} (precipitation time), pH values still in increase with a small change of the resistivity variation speed. The slope changing coincides with the equilibrium pH of calcite variety (Ω = 1.7 slightly higher than 1). The nucleation process becomes more rapid as soon as the equilibrium compared to calcite variety, which is thermodynamically the most stable one, is reached. Given the fact that the resistivity has only changed for the pH exceeding the equilibrium pH of calcite variety, it can be confirmed that the clusters are formed by calcium and carbonate ionic associations such as ionic pairs $CaCO_3^\circ$ often evoked in literature [22,23].
- *Zone 3*: being occurred until the end of the experiment. The slope of resistivity-time curve changes and the resistivity continues increasing rapidly. The related pH values decrease sharply after proton release and during crystalline growth. That is because after precipitation CO_2 formation speed is faster than CO_2 degasification speed by agitation. At supersaturation has been reached (Ω_{prec} = 48), it may appear a new wave of nucleation due to the formation of nucleus in important size in the solution which can justify the important change of the slope.

Therefore, the in–situ measurements of solution resistivity combined with those of pH during the precipitation process, will be helpful in the present study to examine the scale inhibitors effect on calcium carbonate prenucleation stage.

2.5. Conductivity modelling

In a previous study, four conductivity calculation models are used: Kohlrausch [24], Jacobson and Langmuir [25], Laxen [26] and McCleskey et al. [27] methods. Among these models, it has been shown that the one proposed by McCleskey et al is the most suitable for the conductivity calculation. The methodology and basic steps of the curves modelling have been described in detail elsewhere [17].

The electrical conductivity k of a solution for the McCleskey method is calculated as below:

$$k = \sum \lambda_i C_i \tag{7}$$

where C_i is the ion concentration and λ_i is the ionic conductivity calculated as follow:

$$\lambda = \lambda^0(T) - \frac{A(T)I^{1/2}}{1 + BI^{1/2}} \tag{8}$$

where λ^0 and A are function of temperature (°C) and B is an empirical constant.

The resistivity of the solution which is the reciprocal of the electrical conductivity is calculated as below:

$$Resistivity = \frac{1}{k} \tag{9}$$

and

$$\Delta_{Resistivity} = Resistivity(t) - Resistivity(0) \tag{10}$$

3. Results and discussion

3.1. Effect of scale inhibitors on the nucleation threshold

Figs. 4 and 5 report the experimental measurements of pH and $\Delta_{Resistivity}$ during the precipitation tests in absence and presence of RPI and STP. The most useful data are summarized in Table 2.

The presence of scale inhibitors RPI and STP affects remarkably the nucleation kinetic (Figs. 4 and 5). Indeed, t_{prenuc} increases from 12 min in absence of RPI to15 and 20 min in presence of 0.2 and 4 ppm of RPI (Table 2). Moreover, the duration of the prenucleation step ($\Delta t = t_{prec} - t_{prenuc}$) increases from 34 min in absence of RPI to 40 and 190 min in presence of 0.2 and 4 ppm of RPI (Table 2). Thus the duration of the prenucleation step is longer as the inhibitor concentration is higher. Consequently, the distinction between the prenucleation and precipitation thresholds is easier. Liu et al. [28] proved that the nucleation was delayed after the addition of sodium polyacrylate. They supposed that the ionic association of the inhibitor have not interfered with the formation of $CaCO_3$ clusters, but rather they protected them. Also, Clarkson et al. [29] showed that in the absence of triphosphate there was a very short plateau indicating a rapid initial decrease in free calcium concentration, but the presence of the inhibitor increased the length of this plateau from 5 min (without triphosphate) to 30 min (with 10 ppm of triphosphate).

During the prenucleation step and for a concentration of RPI ≤ 14 ppm and STP ≤ 0.8 ppm, a resistivity variation ($\Delta_{Resistivity}$) is detected (Table 2). Indeed, $\Delta_{Resistivity}$ increases from 65 Ω·cm in absence of inhibitor to 160 and to 189 Ω·cm in presence of 4 ppm of RPI and 0.8 ppm of STP, respectively. It is therefore concluded that these substances, without completely inhibiting the formation of ion pairs, act on their rate of formation and consequently influence the nucleation kinetics.

Moreover, the chemical inhibition affects remarkably the saturation state. As seen in Table 2, the supersaturation coefficients increase as inhibitors addition increases until reaching high values for great amounts. Indeed the supersaturation coefficient reached in absence of inhibitor (Ω_{prec} = 48) is multiplied by ~6 in the presence of 4 ppm of RPI (Ω_{prec} = 286) and in presence of only 0.6 ppm of STP (Ω_{prec} = 233). This can be explained by the fact that raising the pH increases and subsequently the Ionic Activity Product (IAP)". The supersaturation coefficient, being equal to the ratio of the IAP by the solubility product, increases with the addition of the inhibitor. Consequently, the maximum supersaturation reached at the initiation time of precipitation is not the direct cause of this precipitation but the consequence of the operating conditions. Thus these substances inhibited the effect of supersaturation on the aggregation rate of the $CaCO_3$ clusters. This can be explained by the fact that the germination requires a low rate of ion pairs when the supersaturation is high. Thus, Table 2 shows that the $\Delta_{Resistivity}$ calculated at the precipitation threshold increases with the amount of inhibitor added. Therefore the metastable state breakdown requires the formation of greater amount of ionic pairs in spite of the strong supersaturation. Since the presence of inhibitor can disadvantages the agglomeration and the coalescence of ions pairs and/or clusters, so that a nuclei can reach a critical size beyond which it can grow up.

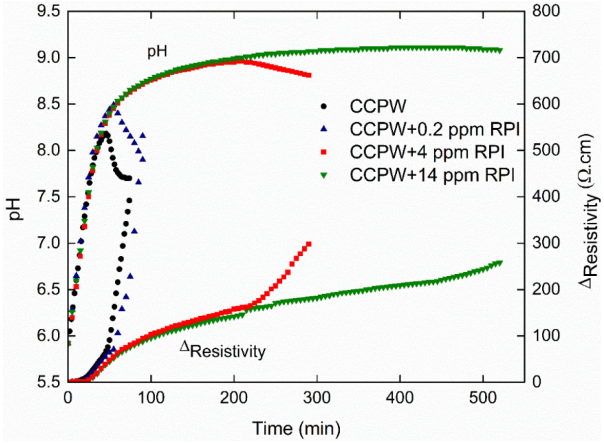

Fig. 4. Temporal evolution of (pH, $\Delta_{Resistivity}$) in absence and presence of RPI at 800 rpm, 30°C and CCPW0.4 g·L^{-1}.

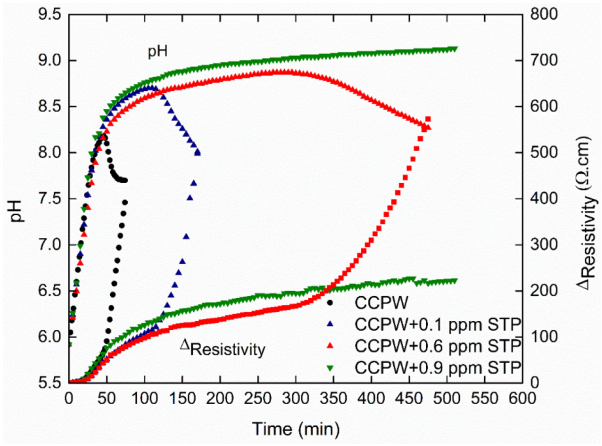

Fig. 5. Temporal evolution of (pH, $\Delta_{Resistivity}$) in absence and presence of STP at 800 rpm, 30°C and CCPW0.4 g·L^{-1}

In addition to their influence on the nucleation thresholds, scale inhibitors affect the adherence of scale on the cell wall. Table 2 shows that the addition of each inhibitor decreases the total precipitated calcium carbonate amounts m_t and increases the mass of calcium carbonate m_w heterogeneously formed on the cell wall. Indeed, m_t passes from 210 mg in the CCPW to 168 and 190 mg for only 4 and 0.6 ppm of RPI and STP, respectively. Moreover m_w passes from 94 mg ($\%_{hete}$ = 45%) in the CCPW to 133 ($\%_{hete}$ = 79%) and 131 ($\%_{hete}$ = 69%) mg for 4 and 0.6 ppm of RPI and STP, respectively. This scaling inhibition confirms previous results on calcium carbonate nucleation obtained by degasification test [30].

3.2. Effect of scale inhibitors on the prenucleation stage

In order to have deeply insight into the effect of scale inhibitors on the nucleation process and more precisely on the prenucleation stage, the resistivity *vs* pH curves were modelled using the McCleskey model.

Table 2
Pre nucleation and precipitation time, supersaturation coefficients and heterogeneous percentage as a function of scale inhibitor amount

Scale inhibitor		t_{prenuc}(min)	t_{prec}(min)	Ω_{prenuc}	Ω_{prec}	Δ Resistivity (Ω·cm)	m_t(mg)	m_w(mg)	% hete (%)
CCPW		12	46	1.7	48	65	210	94	45
RPI (ppm)	0.2	15	55	3	97	77	175	129	74
	4	20	210	5	286	160	168	133	79
	14	20	475	6	405	230	152	138	91
	15	No precipitation detected							
STP (ppm)	0.1	15	110	2.5	157	113	195	129	66
	0.6	20	295	4	233	162	190	131	69
	0.8	20	365	7	353	189	183	128	70
	0.9	No precipitation detected							

During the prenucleation stage and as seen in Figs. 6 and 7, the deviation of curves obtained after inhibitor addition from those of CCPW and McCleskey model starts as soon as the lowest pH values are reached. The prenucleation pH has shifted from 6.73 in absence of inhibitor to 7.20 and to 7.11 in presence of 4 ppm of RPI and 0.6 ppm of STP, respectively. This means that added chemicals delayed ion pair formation as well as higher supersaturation coefficient was required; it has passed from 1.7 to 5 and 4 in presence of 4 ppm of RPI and 0.6 ppm of STP, respectively.

Up to the precipitation pH recorded in absence of inhibitor (pH = 8.18), the effect of STP compared to that of RPI on

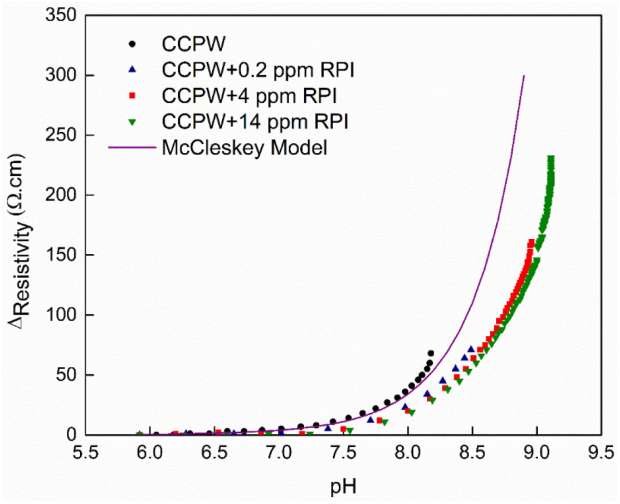

Fig. 6. $\Delta_{Resistivity}$ *vs* pH curves in the prenucleation stage calculated using McCleskey et al. [27] equation and obtained experimentally in a FCP test as a function of RPI dosage at 800 rpm and 30°C.

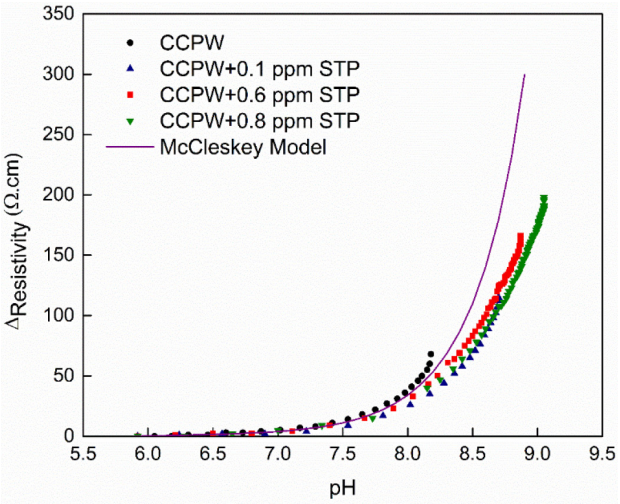

Fig. 7. $\Delta_{Resistivity}$ *vs* pH curves in the prenucleation stage calculated using McCleskey et al. [27] equation and obtained experimentally in a FCP test as a function of STP dosage at 800 rpm and 30°C.

$CaCO_3°$ formation is insignificant (Fig. 7). Given the fact that the nucleation step is not achieved despite the formation of a $CaCO_3°$ content close to that in the absence of inhibitor, we can suggest that the role of STP is limited to reducing the ion pair aggregation rate. Beyond this pH, a neat deviation between theoretical and experimental curves is recorded. This confirms that STP inhibits the association of Ca^{2+} and CO_3^{2-} to form ion pairs. Such behaviour was observed with RPI at lower pH values. The effect of RPI is then more significant on the inhibition of ion pair formation and aggregation (Fig. 6).

3.3. Effect of solution saturation state on the efficiency of scale inhibitor

In the natural water distribution circuits, the supersaturation coefficients remain too low compared to those obtained at laboratory scale; except for the case of cooling towers where degassing is intensive. Therefore, the optimization of an inhibitor is dependent on a good knowledge of the thermodynamic state of the water in the scaled circuit. It is in these extreme conditions of precipitation (Ω_{prec} > 353), at laboratory scale, the content of RPI and STP scalants for a total inhibition of precipitation is 15 and 0.9 ppm, respectively (Table 2). They will be much less important to inhibit scale formation in a natural water circuit for the reasons cited above.

Thus, the experiments are carried out where the saturation state of the water is controlled by stopping the degassing of CO_2 after solution isolation. All the precipitation tests were conducted on 0.4 g·L^{-1} of $CaCO_3$, at 30°C and at 800 rpm in absence or presence of scale inhibitors RPI and STP. At the beginning, the solution was brought to the required pH, which is equal to 7.5 (Ω = 9.95), by magnetic stirring. The cell was then closed hermetically in order to limit CO_2 transfers between liquid and gaseous phases; equilibrium is almost established towards a pH 7.7 corresponding to a supersaturation coefficient Ω = 15.77. Only a slight pH increase of was recorded during the experiment. The most useful data are summarized in Table 3.

Table 3 shows that at the same hydrodynamic conditions and temperature, the $CaCO_3$ precipitation is possible at low supersaturation coefficients. Indeed for a CCPW, Ω_{prec} decreases from 48 to 20 after cell closing. For a 0.2 ppm of RPI, Ω_{prec} decreases from 97 to 33. And for a 0.1 ppm of STP, Ω_{prec} decreases from 157 to 128. Moreover the low supersaturation coefficients require longer time for a massive $CaCO_3$ precipitation. Besides for a CCPW solution, the precipita-

Table 3
Pre nucleation and precipitation time, supersaturation coefficients and heterogeneous nucleation percentage as a function of RPI and STP dosages for a confined cell

Solution		t_{prenuc} (min)	t_{prec} (min)	Ω_{prenuc}	Ω_{prec}	$\%_{hete}$
CCPW		12	105	1.7	20	74
RPI (ppm)	0.2	15	390	3	33	97
	1	–*	–	–	–	–
STP (ppm)	0.1	15	440	3	128	82
	0.6	–*	–	–	–	–

*no precipitation

tion time of opened and confined cell was 46 and 105 min, respectively; here, precipitation was delayed for 59 min. After addition of 0.2 ppm of RPI, the precipitation time of opened and confined cell was 55 and 390 min, respectively, that is, the retarding time of precipitation was 335 min. For treated water with 0.1 ppm STP, the precipitation time of opened and confined cell was 110 and 440 min, respectively. Precipitation was delayed for 330 min.

The precipitation is blocked at very low inhibitor dose (1 ppm for RPI and 0.6 ppm for STP) when the cell is confined (Table 3). Moreover, t_{prec} for an opened cell and for 10 ppm of RPI is equal to 385 min, whereas for a confined cell this same precipitation time is reached for only 0.2 ppm of RPI (Tables 2 and 3). As a consequence the quantity of added RPI is optimized 50 times. Besides, t_{prec} for an opened cell and for 0.83 ppm of STP is 450 min whereas for a confined cell this same t_{prec} is reached for only 0.1 ppm of STP. Thus the quantity of added STP is optimized 9 times. This proves that isolating the cell is very efficient to optimize the quantity of inhibitor used.

As shown in Fig. 8, after an addition of 0.2 ppm of RPI (without cell-closing), the efficiency reaches 50% and from 8 ppm it occurs a blocking of the active sites of calcium carbonate nucleus in growth until reaching 94% as maximum value of efficiency. It should be noted that the retarding effect of RPI, when the working cell is confined, occurs since the addition of small quantity (0.2 ppm). Indeed the corresponding affinity is equal to 94%. Besides, as seen in Fig. 9, when the STP concentration was below 0.5 ppm for an opened cell, poor inhibition efficiency was observed. When the dosage of STP was over 0.6 ppm, the efficiency reaches maximum value of 95%. For a confined cell and up on addition of 0.1 ppm STP, precipitation of $CaCO_3$ was almost completely inhibited. To conclude, the effect of the two inhibitors is more pronounced when the cell is confined because the supersaturation coefficient, the aggregation speed and the $CaCO_3$° quantity are lower than those of the opened cell.

In addition, as seen in Table 3 the greatest heterogeneous percentages are reached when the cell is confined. Indeed

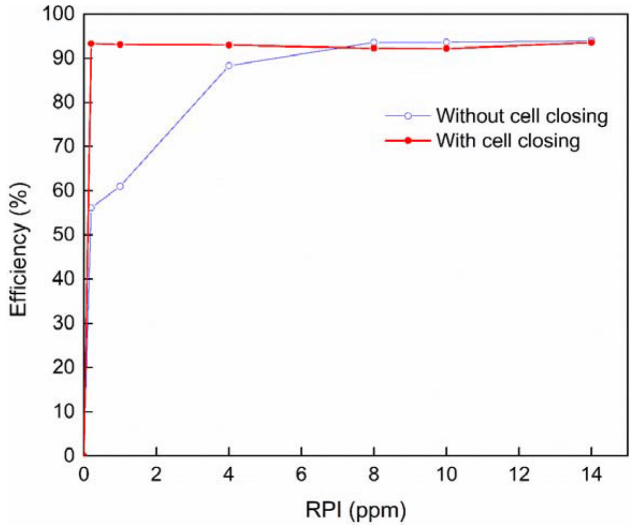

Fig. 8. Variation of the efficiency of inhibition versus dosage of RPI at 800 rpm, 30°C and CCPW0.4 g·L^{-1}.

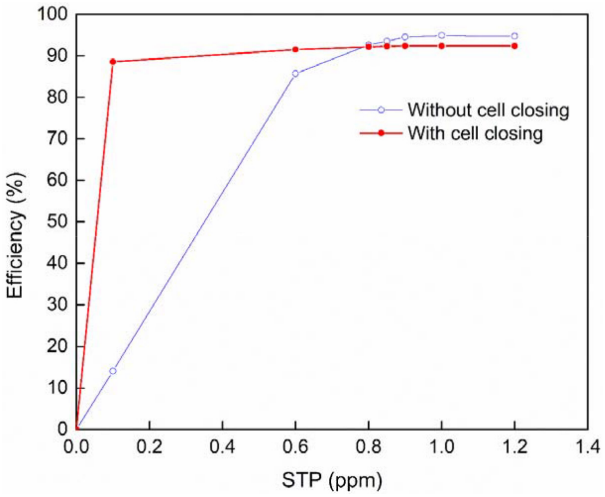

Fig. 9. Variation of the efficiency of inhibition vs. dosage of STP at 800 rpm, 30°C and CCPW0.4 g·L^{-1}.

after confining the cell, $\%_{hete}$ for CCPW solution increases from 45 to 74%. For 0.2 ppm of RPI, it increases from 74 to 97 %. And for 0.1 ppm of STP, it increases from 66 to 82%. Thus closing the cell orientates the adhesion of the formed nucleus of $CaCO_3$ on the walls instead of their formation in the bulk solution.

The experiments show that a best optimization of scale inhibitors used is reliant on a better thermodynamic knowledge of water. As a result, the cost of treatment is reduced and the nature is preserved against these harmful substances.

3.4. Effect of scale inhibitors on the nature of the precipitate formed

In order to have more insight of the effect of each scale inhibitor on the $CaCO_3$ precipitation, the precipitate solid obtained at the end of each FCP test was characterized using the XRD technique. In Figs. 10 and 11 are presented

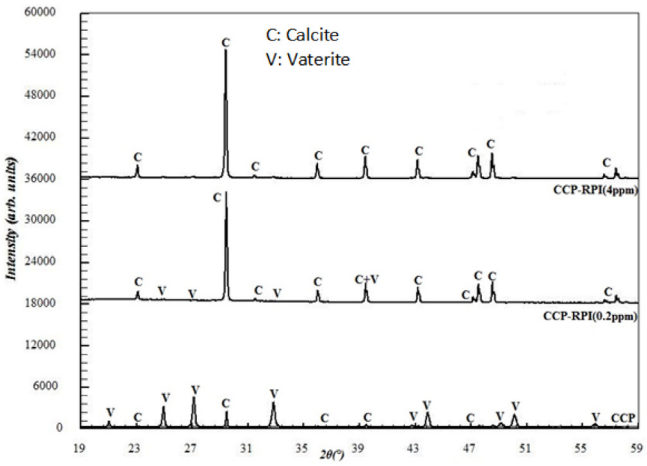

Fig. 10. X-ray diffraction patterns of deposit scale at 30°C obtained in absence and presence of RPI.

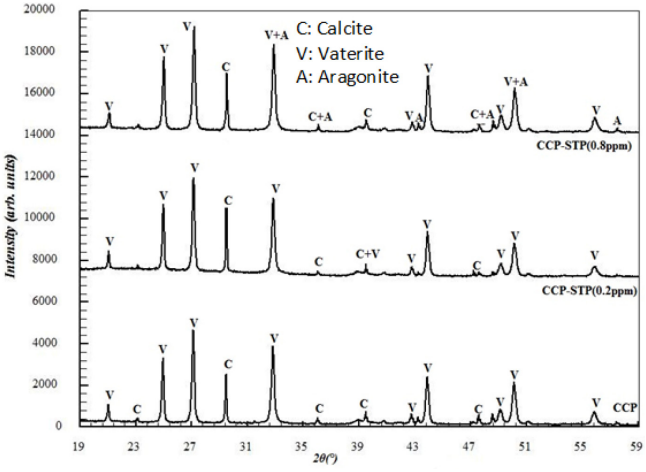

Fig. 11. X-ray diffraction patterns of deposit scale at 30°C obtained in absence and presence of STP.

the XRD patterns of the precipitated obtained in absence and presence of RPI and STP.

The presence of RPI orientates the crystallization towards the formation of the calcite which becomes more and more majority with increasing the inhibitor dose whereas it is the vaterite that was favored in its absence.

In the case of precipitate formed in the presence of STP, this inhibitor seems to not influence the phases formed; vaterite remains the majority regardless of the STP content.

These results may suggest that the modes of action of these two inhibitors on the nucleation-precipitation of $CaCO_3$ are different.

4. Conclusion

In the present study, an accelerated scaling method, based on electrical conductivity modelling applied to the FCP method data, was used to assess the scale inhibitors effect on calcium carbonate prenucleation stage. Tested solutions are calco-carbonic pure waters.

The presence of scale inhibitors RPI and STP affects remarkably the nucleation kinetic. Thus the distinction between the prenucleation and precipitation thresholds is easier for a higher dose of inhibitor. Indeed, the chemical inhibition increases the quantity of the nucleus formed and thus the duration of each nucleation phase is prolonged. The resistivity curves show that breaking the metastable state requires the formation of larger amounts of ion pairs. This suggests that the presence of the inhibitor delays the start of the agglomeration and the coalescence of ion pairs so that a nuclei can reach a critical size beyond which it can grow up. In addition, these substances inhibited the role of supersaturation on the aggregation rate of the $CaCO_3$ clusters because the germination requires a low rate of ion pairs for high supersaturations to take place. Moreover, the chemical inhibition promotes preferentially the heterogeneous nucleation detrimentally to the scaling in the bulk solution. Besides, the inhibitors act to prevent the association of Ca^{2+} and CO_3^{2-} to form ion pairs. This effect is more marked with the organic RPI inhibitor than that of the STP. Additionally, the effect of the two inhibitors is more pronounced when the cell is confined because the blocking of calcium carbonate growth nucleation was happened for lower dosage. Finally, on the micro structural level, the presence of RPI favors calcite at the expense of vaterite. However, the STP did not greatly influence the micro structure of the formed scale.

References

[1] F. Alimi, M. Tlili, M.B. Amor, C. Gabrielli, G. Maurin, Influence of magnetic field on calcium carbonate precipitation, Desalination, 206 (2007) 163–168.
[2] L. Zhu, Y. Han, C. Zhang, R. Zhao, S. Tang, Molecular dynamics simulation for the impact of an electrostatic field and impurity Mg^{2+} ions on hard water, RSC Adv., 7 (2017) 47583–47591.
[3] C. Ruiz-Agudo, C.V. Putnis, A. Ibañez-Velasco, E. Ruiz-Agudo, A. Putnis, A potentiometric study of the performance of a commercial copolymer in the precipitation of scale forming minerals, Cryst. Eng. Comm., 18 (2016) 5744–5753.
[4] H. Huang, Q. Yao, B. Liu, N. Shan, H. Chen, Synthesis and characterization of scale and corrosion inhibitors with hyperbranched structure and the mechanism, New J. Chem., 41 (2017) 12205–12217.
[5] S.B. Ahmed, M. Tlili, M.B. Amor, H.B. Bacha, B. Elleuch, Calcium sulphate scale prevention in a desalination unit using the SMCEC technique, Desalination, 167 (2004) 311–318.
[6] M.M. Tlili, A.S. Manzola, M. Ben Amor, Optimization of the preliminary treatment in a desalination plant by reverse osmosis, Desalination, 156 (2003) 69–78.
[7] G. Liu, M. Xue, Q. Liu, H. Yang, J. Yang, Y. Zhou, Maleic anhydride-allylpolyethoxy carboxylate copolymer as an effective and environmentally benign inhibitor for calcium carbonate in industrial cooling systems, RSC Adv., 7 (2017) 24723–24729.
[8] S.L.P. Wolf, K. Jähme, D. Gebauer, Synergy of Mg^{2+} and poly(aspartic acid) in additive-controlled calcium carbonate precipitation, Cryst. Eng. Comm., 17 (2015) 6857–6862.
[9] E.G. Darton, Scale inhibition techniques used in membrane systems, Desalination, 113 (1997) 227–229.
[10] W.N. Al Nasser, F.H. Al-Salhi, M.J. Hounslow, A.D. Salman, Inline monitoring the effect of chemical inhibitor on the calcium carbonate precipitation and agglomeration, Chem. Eng. Res. Des., 89 (2011) 500–511.
[11] Q. Yang, Y. Liu, A. Gu, J. Ding, Z. Shen, Investigation of calcium carbonate scaling inhibition and scale morphology by AFM, J. Colloid Interface Sci., 240 (2001) 608–621.
[12] Y.P. Lin, P.C. Singer, G.R. Aiken, Inhibition of calcite precipitation by natural organic material: Kinetics, mechanism, and thermodynamics, Environ. Sci. Technol., 39 (2005) 6420–6428.
[13] D. Liu, W. Dong, F. Li, F. Hui, J. Lédion, Comparative performance of polyepoxysuccinic acid and polyaspartic acid on scaling inhibition by static and rapid controlled precipitation methods, Desalination, 304 (2012) 1–10.
[14] L.F. Greenlee, F. Testa, D.F. Lawler, B.D. Freeman, P. Moulin, The effect of antiscalant addition on calcium carbonate precipitation for a simplified synthetic brackish water reverse osmosis concentrate, Water Res., 44 (2010) 2957–2969.
[15] M.M. Tlili, M.B. Amor, C. Gabrielli, S. Joiret, G. Maurin, P. Rousseau, Characterization of $CaCO_3$ hydrates by micro-Raman spectroscopy, J. Raman Spectrosc., 33 (2002) 10–16.
[16] M.M. Tlili, Etude des mécanismes de précipitation du carbonate de calcium. Application à l'entartrage, in, University of Paris 6, 2002.
[17] R. Hamdi, M.M. Tlili, Conductometric study of calcium carbonate prenucleation stage: underlining the role of $CaCO_3^o$ ion pairs, Cryst. Res. Technol., 51 (2016) 99–109.
[18] Y. Chao, O. Horner, P. Vallée, F. Meneau, O. Alos-Ramos, F. Hui, M. Turmine, H. Perrot, J. Lédion, In situ probing calcium carbonate formation by combining fast controlled precipitation method and small-angle X-ray scattering, Langmuir, 30 (2014) 3303–3309.

[19] R. Hamdi, M. Khawari, F. Hui, M. Tlili, Thermodynamic and kinetic study of $CaCO_3$ precipitation threshold, Desal. Water Treat., 57 (2016) 6001–6006.
[20] A. Fathi, T. Mohamed, G. Claude, G. Maurin, B.A. Mohamed, Effect of a magnetic water treatment on homogeneous and heterogeneous precipitation of calcium carbonate, Water Res., 40 (2006) 1941–1950.
[21] M.B. Amor, D. Zgolli, M.M. Tlili, A.S. Manzola, Influence of water hardness, substrate nature and temperature on heterogeneous calcium carbonate nucleation, Desalination, 166 (2004) 79–84.
[22] J.-Y. Gal, Y. Fovet, N. Gache, Mechanisms of scale formation and carbon dioxide partial pressure influence. Part II. Application in the study of mineral waters of reference, Water Res., 36 (2002) 764–773.
[23] D. Genovese, M. Montalti, F. Otálora, J. Gómez-Morales, M. Sancho-Tomás, G. Falini, J.M. García-Ruiz, Role of CaCO3° neutral pair in calcium carbonate crystallization, Cryst. Growth Des., 16 (2016) 4173–4177.
[24] F. Kohlrausch, The resistance of the ions and the mechanical friction of the solvent, Proceedings of the Royal Society of London, 71 (1902) 338–350.
[25] R.L. Jacobson, D. Langmuir, Dissociation constants of calcite and $CaHCO_3^+$ from 0 to 50°C, Geochim. Cosmochim. Acta, 38 (1974) 301–318.
[26] D.P.H. Laxen, A specific conductance method for quality control in water analysis, Water Res., 11 (1977) 91–94.
[27] R.B. McCleskey, D.K. Nordstrom, J.N. Ryan, J.W. Ball, A new method of calculating electrical conductivity with applications to natural waters, Geochim. Cosmochim. Acta, 77 (2012) 369–382.
[28] J. Liu, S. Pancera, V. Boyko, J. Gummel, R. Nayuk, K. Huber, Impact of sodium polyacrylate on the amorphous calcium carbonate formation from supersaturated solution, Langmuir, 28 (2012) 3593–3605.
[29] J.R. Clarkson, T.J. Price, C.J. Adams, Role of metastable phases in the spontaneous precipitation of calcium carbonate, J. Chem. Soc. Faraday Trans., 88 (1992) 243–249.
[30] I. Ben salah, M.M. Tlili, M. Ben Amor, Influence of foreign salts to the $CaCO_3$–CO_2–H_2O system and antiscalants on the adherence of calcium carbonate on the stainless steel, Eur. J. Water Qual., 41 (2010) 51–66.